Chemical Methodologies 6(2022) 74-82

Chemical Methodologies

Journal homepage: http://chemmethod.com

Original Research Article

Conducting Poly[*N*-(4-Methoxy Phenyl)Maleamic Acid]/Metals Oxides Nanocomposites for Corrosion Protection and Bioactivity Applications

Rawaa Abbas Mohammed*, Khulood A. Saleh

Department of Chemistry, College of Science, University of Baghdad, Baghdad, Iraq

ARTICLE INFO

Article history

Submitted: 2021-09-19
Revised: 2021-10-04
Accepted: 2021-10-20
Manuscript ID: CHEMM-2109-1383
Checked for Plagiarism: **Yes**
Language Editor:
Dr. Behrouz Jamalvandi
Editor who approved publication:
Dr. Mohsen Oftadeh

DOI: 10.22034/chemm.2022.1.8

KEYWORDS

Inhibition efficiency
Nanoparticles
Electrochemical polarization
Low carbon steel

ABSTRACT

Corrosion is considered as the most common cause of steel material property degradation, while coatings are effective and popular corrosion protection methods. Coatings come in a variety of forms, each with its own set of effectiveness, methods and constituents. This study used an electrochemical oxidation approach to make Poly [N-(4-Methoxy Phenyl) maleamic acid] from monomer [N-(4-Methoxy Phenyl) maleamic acid] (NPM) in a 3.5% seawater solution. On a low carbon steel [L.C.S] electrode (working electrode), a polymer film was produced. The polymer was created, according to infrared, SEM and FTIR examinations. Using the electrochemical polarization approach, the anticorrosion function of polymer films on L.C.S was examined. Also, adding nanoparticles (NP), like CuO and ZnO to the monomer solution improved the polymers anticorrosion. The results revealed that there was an increase in the L.C.S corrosion rate with the increase of temperature from 293K to 323K, while the values related to coatings polymer inhibition efficiency improved with NPs addition. For the corrosion of L.C.S in salt medium prior to and following polymeric coating, thermodynamic and kinetic activation parameters were estimated. The impact of preparing polymers on certain bacteria strains was also investigated.

GRAPHICAL ABSTRACT

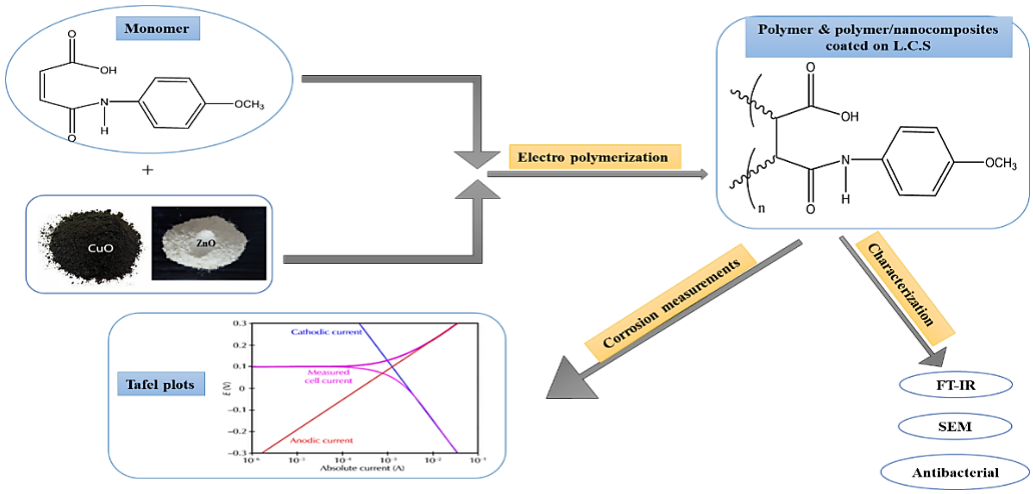

* Corresponding author: Rawaa Abbas Mohammed
E-mail: rawaa.a.mohammed@sc.uobaghdad.edu.iq

Introduction

For industrial and construction development, metallic corrosion is a severe economic and safety issue [1]. Inorganic coatings [2-4], organic coatings [5], corrosion inhibitors [6], and ceramic coatings [7, 8] are only a few of the techniques to corrosion protection that have been developed. Organic coatings have lately drawn a lot of attention because of their low cost, ease of application, and functional potential, so they have become one of the most effective corrosion protection techniques. Typically, corrosion protection is provided by organic polymeric coatings that establish a barrier between a metal and its surrounding environment. All polymeric coatings, on the other hand, are permeable to corrosive species like water, oxygen, and chloride ions. The permeability enhances the process of corrosion initiation and reduces the polymeric coating's service time. Incorporating inorganic fillers into the polymeric coating formulation may help to decrease permeability and extend the composite coating's lifespan. Inorganic nano-fillers, in particular, have better barrier characteristics than traditional fillers because of their high boundary volume and fine gain size [9-11]. Good adhesion, long-term corrosion resistance, high surface mechanical abrasion and good durability are all desirable qualities in a coating. It has been demonstrated that the use of NPs in conducting polymer coatings can enhance electrochemical anticorrosion and other properties like thermal stability, adhesion, hydrophobic property, mechanical strength, and magnetostatic shielding [12-15]. As a result, various types of NPs including Zn, TiO_2, Si, ZnO, Al_2O_3, SiO_2, CuO and CeO_2 have been added in polymer coatings and have shown superior protective behavior compared to normal polymer coatings. CuO and ZnO NPs have been examined as additives in conducting polymer coatings.

In this work, polymers were synthesized to prevent corrosion of L.C.S by using electro polymerization of conducting polymer coatings and polymer nanocomposites with ZnO & CuO NPs and their corrosion protection performance in seawater at different temperatures were evaluated [293-323] K.

Material and methods

Experimental

The NPM's electrochemical polymerization onto the anode electrode surface of L.C.S was performed in a potentiostat with regulated DC power supply as scheme 1. Acetone was used for cleaning and washing the specimens. The polymerization solutions were 0.1g *N*-(4-Methoxy Phenyl) Maleamic acid (monomer) [16] in 100 ml H_2O with 5 drops of H2SO4 concentration [98%]. At room temperature and 1.1V, the polymerization took place. At the anode's surface, a polymer film was deposited. L.C.S was employed for corrosion measurements. The sheet was mechanically cut into coupons with dimensions of [2.5 cm * 2 mm] apiece. After washing with ethanol, each one of the coupons was degreased. Prior to usage, the washed sample was dipped in acetone and left to dry in the air. In addition, the auxiliary electrode was the platinum, the working electrode was the L.C.S and reference electrode was saturated calomel electrode [SCE]. Under potentiostatic circumstances, cathodic and anodic polarization of L.C.S was conducted in [3.50% NaCl] solution in the presence and absence of a coated layer. Furthermore, all experiments were conducted at various temperatures [293-323] K. In addition, 0.04 g of CuO (99%, 40 nm) and ZnO (99%, 10-30 nm) NPs were present, which helped to strengthen the coated layers to bacterial and corrosion.

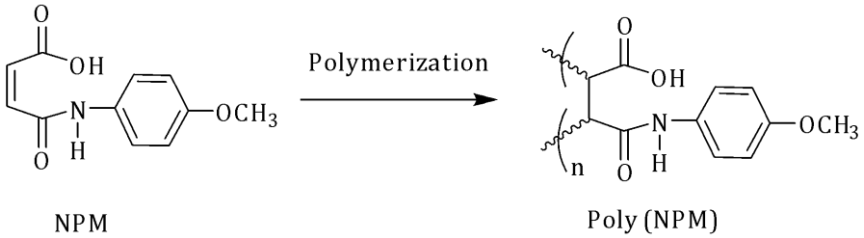

Scheme 1: Polymerization of the monomer to polymer

Result and Discussion

A cationic [17,18] mechanism might be suggested for explaining the electro polymerization reactions, specifically the grafting and growth of Poly (NPM) films, depending on the existing literature. The introduction of an anodic potential to an NPM solution in the cationic mechanism (Scheme 2) results in the transfer of an electron from monomer to working electrode [A 1]. The transfer in the adsorption of a radical-cation on electrode surface happens, as shown in [A 2]. Alternatively, in the case where [A2] has a long enough lifetime relative to the time it takes for an NPM molecule to diffuse toward the electrode, NPM molecules might add on through a cationic mechanism at the charged ends regarding the adsorbed oxidized NPM [A4]. The creation of a grafted polymer [pale brownish] is the result of such propagation process.

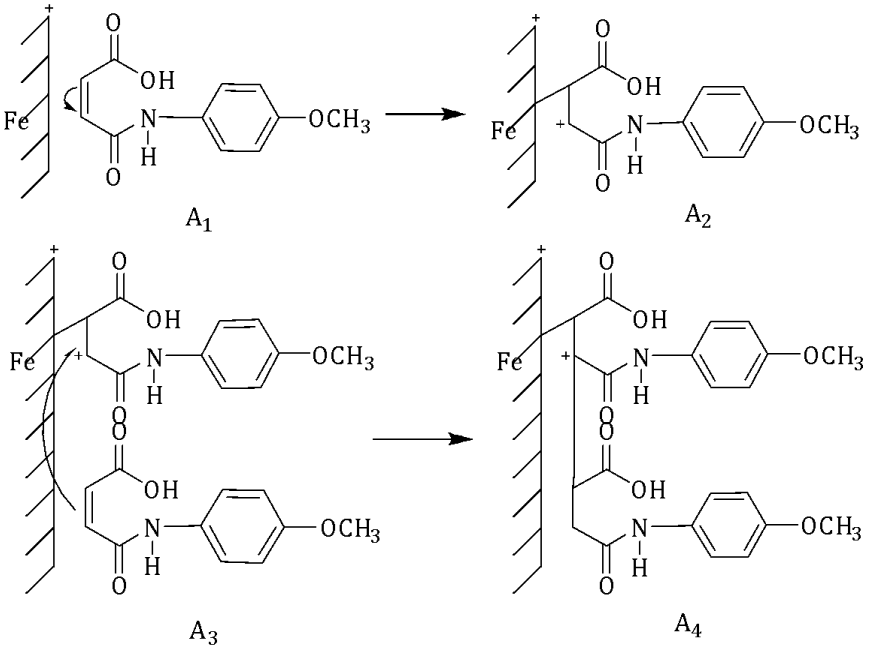

Scheme 2: Proposed Cationic Mechanism for Grafting and Growth of the poly (NPM) film

Structure of Poly (NPM)

Figure 1 shows the FTIR spectra regarding a Poly (NPM) coating film made from NPM. The characteristic NPM bands in Figure 1, double bond C=C 3070 cm^{-1}, have vanished in this spectrum, confirming the production of Poly (NPM). Since the polymer has a wide chain length distribution, the bands are fairly broad.

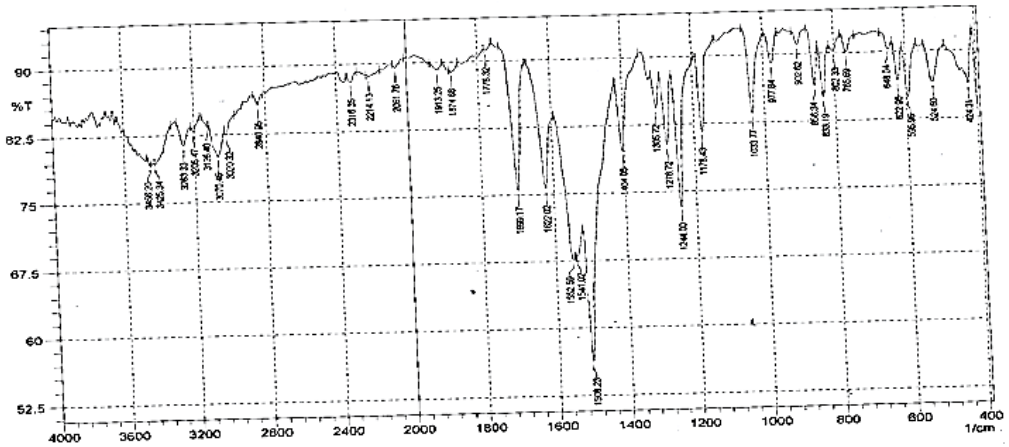

Figure 1: FTIR spectra of NPM

The existence of C=O carboxyl group was established by the band appearing at 1641.31 cm-1, the absorption related to amide group at 3454.27 cm^{-1}, and the absorption bonds of the O-H carboxylic group at 2500-3200 cm^{-1} [19,20]; the transmission peaks are illustrated in Table 1.

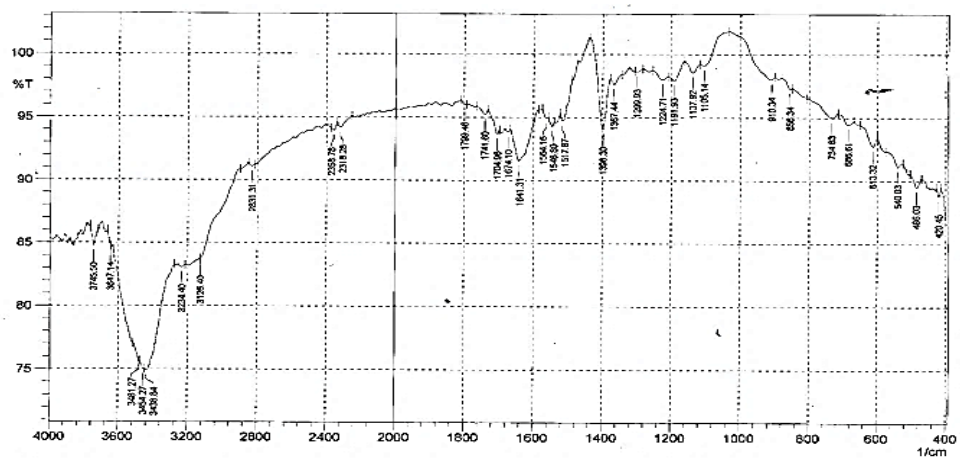

Figure 2: FTIR spectra of Poly (NPM)

Table1: FTIR data for Poly (NPM)

For monomer & polymer	
Organic functional group	**Wave number (cm^{-1})**
C=C alkene group	3070
C=O carboxylic group	1641.31
N-H amide group	3454.27
O-H carboxylic group	2500-3200

Surface Morphological Studies

SEM was utilized to examine the surface morphology related to the polymer as well as its nanocomposite coatings on L.C.S. Also, SEM images of the pure polymer and its nanocomposites are shown in Figures 3A, 3B, and 3C. SEM scans demonstrated that ZnO NPs have a significant impact on the polymer's morphology, whereas CuO NPs have a spherical shape and appear to form clusters [21]. The pure polymer morphology (Figure 3A) differs significantly from the morphology of its nanocomposites (Figure 3B and 3C) in SEM micrographs. The nanocomposites revealed growth of a chain pattern of the polymer with NPs between the junctions of the polymer chain network, while the polymer with no NPs displayed short nano-fibers in the network form. The NPs in nanocomposites are distributed evenly throughout polymer matrix. NPs are nearly global, uniform and agglomerated slightly [22].

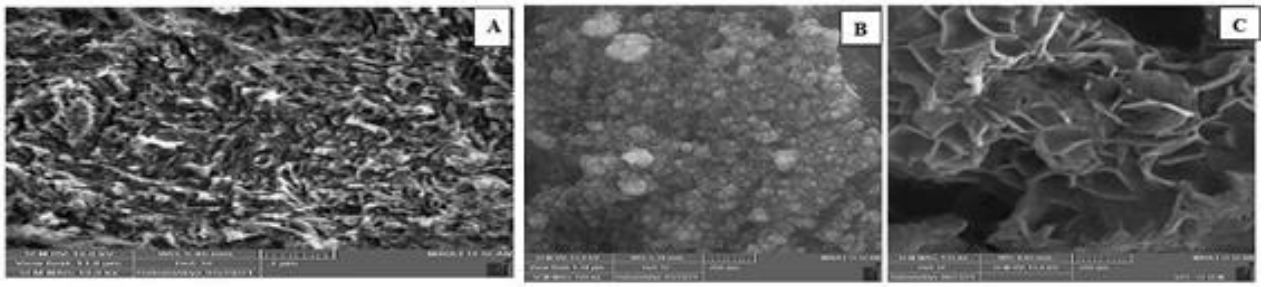

Figure 3: SEM images of [A] Poly (NPM), [B] Poly (NPM)/CuO nanocomposite and [C] Poly (NPM)/ZnO nanocomposite

Anticorrosion behavior

At various temperatures [293-323] K, the impact of a polymeric coating film on cathodic and anodic polarization curves of L.C.S in 3.50% NaCl solution was investigated. Figure 4 shows the impact of introducing various NPs [CuO and ZnO]. Extrapolation of cathodic and anodic Tafel lines yielded corrosion current density (Icorr). The impact of polymer coatings without and with NPs on the corrosion characteristics of L.C.S electrode in seawater solution is shown in Table 2. Cathodic Tafel slope (bc), corrosion current (Icorr), anodic Tafel slope (ba), corrosion potential (Ecorr), weight (W.L), inhibition efficiency (IE), and

penetration loss (P.L) are those parameters. Scheme 1 was used to compute inhibition efficiency from corrosion current densities [23]:

$$\% IE = (1 - \frac{Icorr}{I^o corr}) * 100 \qquad 1$$

Where Iocorr and Icorr are the corrosion rates of L.C.S electrode in absence and presence of coatings, respectively.

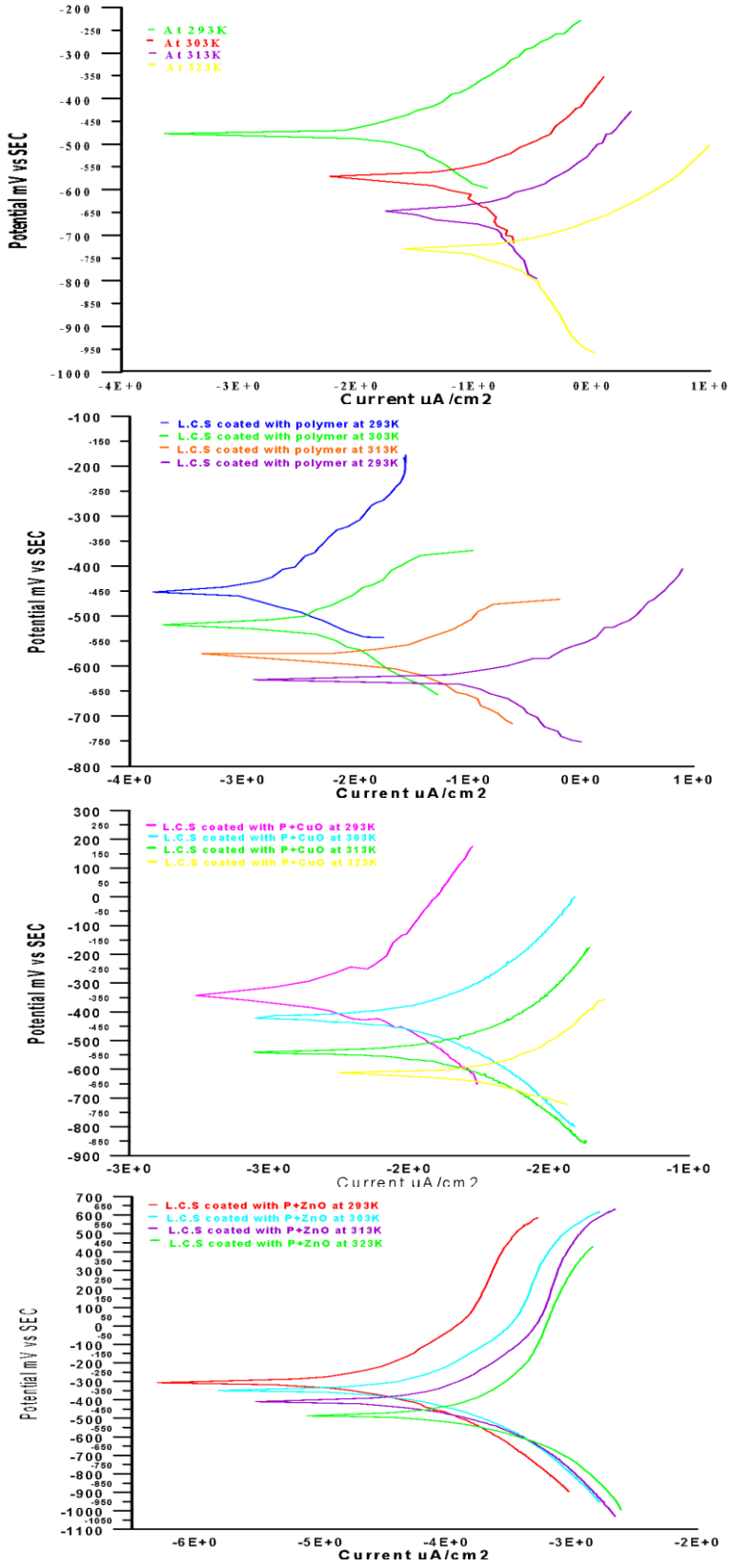

Figure 4: Polarization curves of L.C.S coated with polymer and nanoparticles in 3.5% seawater at different temperatures

In the case when nanomaterials were added to the monomer solution, the corrosion potential switched to more positive values and Icorr reduced, showing that such particles have an inhibitory impact. The corrosion potential switched to the noble side in the case when the polymer film was constructed with nanomaterial coated on L.C.S. This shows a film created on the metal surface's anodic sites [24].

Table 2: Corrosion data of L.C.S in 3.5% seawater with and with no coatings

T(K)		*E_{corr} (mV)*	*I_{corr} (μA/cm²)*	*Bc (mV/De)*	*ba (mV/De)*	*W.L (g/m².d)*	*P.L (mm/)*	*IE%*	*R_p (Ω/cm²)*
Uncoated L.C.S	293	-471.8	24.1	-136.4	130.7	4.02	0.187	-	1202.6
	303	-572.1	79.7	-162.6	132.7	14.30	0.664	-	398.1
	313	-646.5	111.3	-186.7	148.5	28.70	1.330	-	322.7
	323	-676.8	133.2	-193.9	131.6	32.20	1.540	-	255.6
Coated L.C.S with polymer	293	-452.1	3.3	-79.4	123.7	0.27	0.0127	86.3	6363.2
	303	-513.0	11.9	-109.2	113.6	0.50	0.0231	85.1	2031.6
	313	-581.1	18.0	-138.1	121.0	0.61	0.0521	83.8	1555.8
	323	-631.0	25.5	-137.6	97.0	0.83	0.0759	80.9	968.8
Coated L.C.S with polymer + CuO	293	-325.0	1.3	-119.8	110.6	0.0176	0.0004	94.6	19208.4
	303	-524.8	7.2	-268.5	276.8	0.0290	0.0005	91.0	8219.6
	313	-601.9	12.8	-239.6	260.7	0.0373	0.0008	88.5	4235.4
	323	-610.3	19.9	-228.3	262.7	0.0444	0.0011	85.1	2665.2
Coated L.C.S with polymer + ZnO	293	-310.0	0.290	-472.3	580.6	0.0069	0.0003	98.8	389956.3
	303	-350.7	0.372	-497.3	609.3	0.0088	0.0004	99.5	321338.9
	313	-422.5	0.533	-524.1	685.7	0.0120	0.0006	99.5	243368.8
	323	-508.1	0.764	-461.9	588.9	0.0183	0.0009	99.4	147123.5

Kinetic and Thermodynamic of Activation Parameters

The corrosion reaction could be indicated as Arrhenius-type process, this rate has been given by equation 2 [25]:

$$C.R = A\ exp\left(\frac{-Ea}{RT}\right) \qquad 2$$

In which [A] represents Arrhenius pre-exponential constant, [Ea] denotes activation corrosion energy for corrosion process, [T] represents absolute temperature and [R] represents universal gas constant. Figure 5 illustrates Arrhenius plots regarding the logarithm of the corrosion current density vs 1/T, for 3.5% seawater, with and without polymer and NPs coating. The [Ea] values were determined from slopes regarding such plots and were evaluated, as presented in Table 3. Furthermore, the values of activation entropy [ΔS*] and enthalpy of activation [ΔH*] were acquired from Figure 6, from transition states equation 3 [26]:

$$C.R = \frac{RT}{Nh}\ exp\ exp\left(\frac{\Delta S^*}{R}\right)\ exp\ exp\left(\frac{-\Delta H^*}{RT}\right) \qquad 3$$

In which [h] represents the Planck's constant, and [N] represents the Avogadro's number. A plot of Log (C.R/T) as a function of 1/T was made and straight lines were acquired. [ΔS*] and [ΔH*] were evaluated from slope and intercept respectively from linear plot, as presented in Table 2.

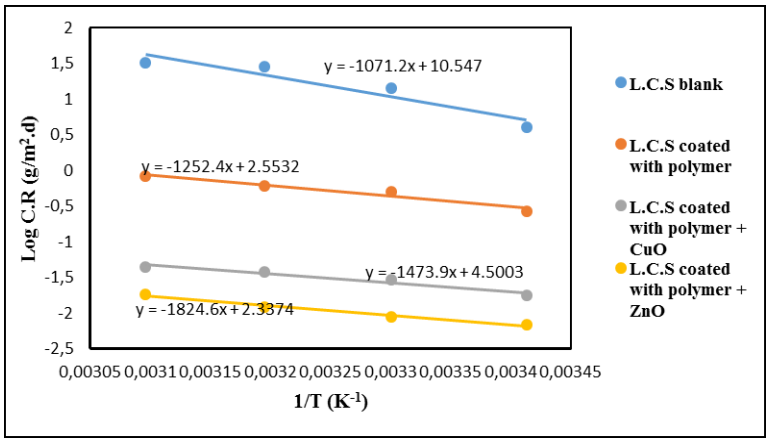

Figure 5: Arrhenius Plots of log C.R versus 1/T for L.C.S in 3.5% seawater in the absence and presence coatings

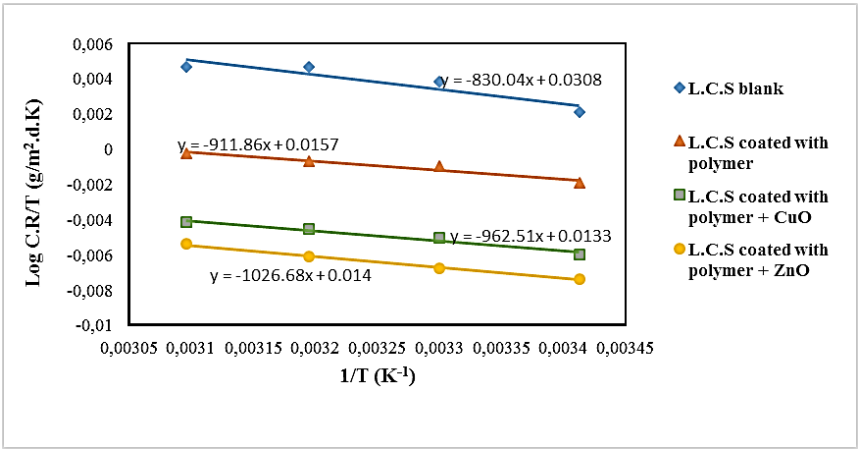

Figure 6: Arrhenius plots of log C.R/T versus 1/T for L.C.S in 3.5% seawater in absence and presence coatings

Table 3: Kinetic & thermodynamic data at different temperatures for the L.C.S in 3.5% seawater with and without coatings

Coating	*R^2*	*Ea (kJ.mole^{-1})*	*R^2*	*ΔH* (kJ.mol^{-1})*	*ΔS* (J.mol-1.K^{-1})*
Uncoated L.C.S	0.8968	20.5	0.8352	15.9	-196.9
Coated L.C.S with polymer	0.9551	24.0	0.9494	17.5	-197.2
Coated L.C.S with polymer + CuO	0.9542	28.2	0.9690	18.4	-197.3
Coated L.C.S with polymer + ZnO	0.9769	34.9	0.9928	19.7	-197.3

The inhibition efficiency of L.C.S increased after coatings and its increase resulted in the increase of the apparent activation corrosion energy. The positive sign of ΔH* reflects endothermic nature of L.C.S dissolution process in presence and absence of coating film, whereas the negative sign of ΔS* exhibits a system disorder decrease [27,28].

Antibacterial Study

Due to the reemergence of infectious illnesses and the creation of antibiotic-resistant strains, nanotechnology has become increasingly significant in the pharmaceutical and bio-medical fields as one of the alternative antimicrobial strategies [29]. The biocidal efficiency of NPs is thought to be due to a combination of their high surface to volume ratio and small size, allowing for close contacts with microbial membranes [30]. Table 4 shows the results regarding the antibacterial activity of polymer and polymer containing NPs. According to the results, the polymer and polymer containing NPs have excellent activity against Escherichia coli and Staphylococcus aureus. As an antibacterial agent, such metal oxides have received a lot of attention. CuO and ZnO, for example, prevent Escherichia coli and Staphylococcus aureus internalization and adhesion [31,32].

Table 4: Antimicrobial activities of tested polymer and polymer with nanoparticles. The inhibition zone measured by (mm)

coating	E. coli	Staph. aureus
Poly(NPM)	11 mm	10mm
Poly(NPM)/CuO NPs	13 mm	14 mm
Poly(NPM)/ZnO NPs	14mm	20mm

Conclusion

The corrosion rate in seawater solution has been shown to be inhibited by electro polymerization related to NPM on L.C.S surface. FT-IR analysis validated the polymer's synthesis. When nanomaterials are added to a monomer solution, particularly ZnO NPs, the inhibitory efficiency of the polymer increases to more than 99%. Polymer coatings might give antimicrobial activities against E. coli and S. aureus bacteria in addition to corrosion resistance, while Poly

(NPM)/nanocomposites displayed active bacterial resistance against Staph. Aureus and E. coli organisms when compared with pure polymer. Electro polymerization protective coatings will have a more practical and a wider applicability with more research into the method and associated characterization methods.

Funding

This research did not receive any specific grant from funding agencies in the public, commercial, or not-for-profit sectors.

Authors' contributions

All authors contributed toward data analysis, drafting and revising the paper and agreed to be responsible for all the aspects of this work.

Conflict of Interest

We have no conflicts of interest to disclose.

ORCID

Rawaa Abbas Mohammed:

https://www.orcid.org/000-567-5679-5677

Khulood A. Saleh:

https://www.orcid.org/000-567-5678-5978

References

[1]. George, F., Hays P., *Now is the Time. World Corrosion Organization*: New York, NY, USA, 2016 [Google Scheme]

[2]. Li, P., He X., Huang T.C., White K.L., Zhang X., Liang H., Nishimura R., Sue H.J., *J. Mater. Chem.*, 2015, **3**:2669 [Crossref], [Google Scheme], [Publisher]

[3]. Huang, B.S., Lai G.H., Yang T.I., Tsai M.H., Chou Y.C., *Polymers*, 2020, **12**:91. [Crossref], [Google Scheme], [Publisher]

[4]. Lai, G., Huang T.C., Tseng I.H., Huang B.S., Yang T.I., Tsai M.H., *Express Polym. Lett.*, 2019, **13** [Crossref], [Google Scheme]

[5]. Liang, J., Srinivasan P.B., Blawert C., Dietzel W., *Corros. Sci.*, 2009, **51**:2483 [Crossref], [Google Scheme], [Publisher]

[6]. Xiang, N., Song R.G., Zhuang J.J., Song R.X., Lu X.Y., Su X.P., *T. NONFERR. METAL. SOC.*, 2016, **26**:806 [Crossref], [Google Scheme], [Publisher]

[7]. Anitha, R., Chitra S., Hemapriya V., Chung I.M., Kim S.H., Prabakaran M., *Constr. Build. Mater.*, 2019, **213**:246 [Crossref], [Google Scheme], [Publisher]

[8]. Ituen, E.B., Akaranta O., Umoren S.A., *J. Mol. Liq.*, 2017, **246**:112 [Crossref], [Google Scheme], [Publisher]

[9]. Keyoonwong, W., Guo Y., Kubouchi M., Aoki S., Sakai T., *Int. J. Corros.*, 2012 [Crossref], [Google Scheme], [Publisher]

[10]. Motte, C., Poelman M., Roobroeck A., Fedel M., Deflorian F., Olivier M.G., *Prog. Org. Coat.*, 2012, **74**:326 [Crossref], [Google Scheme], [Publisher]

[11]. Huttunen-Saarivirta, E., Vaganov G.V., Yudin V.E., Vuorinen J., *Prog. Org. Coat.*, 2013, **76**:757 [Crossref], [Google Scheme], [Publisher]

[12]. Yakovenko, O.S., Matzui L.Y., Vovchenko L.L., Trukhanov A.V., Kazakevich I.S., Trukhanov S.V., Prylutskyy Y.I., Ritter U., *J. Mater. Sci.*, 2017, **52**:5345 [Crossref], [Google Scheme], [Publisher]

[13]. Mostafaei, A., Nasirpouri F., *Prog. Org. Coat.,* 2014, **77**:146 [Crossref], [Google Scheme], [Publisher]

[14]. Hosseini, M.G., Aboutalebi K., *Prog. Org. Coat.*, 2018, **122**:56 [Crossref], [Google Scheme], [Publisher]

[15]. Ramezanzadeh, B., Bahlakeh G., Ramezanzadeh M., *Corros. Sci.*, 2018, **137**:111 [Crossref], [Google Scheme], [Publisher]

[16]. Ali, F.M., Kadem K.J., Rahi F.A., Gayadh E.W., *ANJS*, 2014, **17**:1 [Crossref], [Google Scheme], [Publisher]

[17]. Younang, E., Léonard-Stibbe E., Viel P., Defranceschi M., Lécayon G., Delhalle J., *Mol. Eng.*, 1992, **1**:317 [Crossref], [Google Scheme], [Publisher]

[18]. Léonard-Stibbe, E., Lécayon G., Deniau G., Viel P., Defranceschi M., Legeay G., Delhalle J., *J. Polym. Sci. A Polym. Chem.*, 1994, **32**:1551 [Crossref], [Google Scheme], [Publisher]

[19]. Silverstein, R.M., Bassler G.C., *J. Chem. Educ.*, 1962, **39**:546. [Crossref], [Google Scheme], [Publisher]

[20]. Koj, N., *Infrared abstraction spectroscopy. Nankodo Company Limited*, Tokyo, 1962. [Crossref], [Google Scheme], [Publisher]

[21]. Sackey, J., Nwanya A., Bashir A.K., Matinise N., Ngilirabanga J.B., Ameh A.E., Coetsee E., Maaza

M., *Mater. Chem. Phys.*, 2020, **244**:122714. [Crossref], [Google Scheme], [Publisher]
[22]. Mobin, M., Aslam J., Alam R., *Arab. J. Sci. Eng.*, 2017, **42**:209 [Crossref], [Google Scheme], [Publisher]
[23]. Yoo, S.H., Kim Y.W., Chung K., Baik S.Y., Kim J.S., *Corros. Sci.*, 2012, **59**:42 [Crossref], [Google Scheme], [Publisher]
[24]. Raja, A.S., Rajendran S., *J. Electrochem. Sci. Eng.*, 2012, **2**:91 [Crossref], [Google Scheme]
[25]. Bentiss F., Traisnel M., Chaibi N., Mernari B., Vezin H., Lagrenée M., *Corros. Sci.*, 2002, **44**:2271 [Crossref], [Google Scheme], [Publisher]
[26]. Umoren S.A., Obot I.B., Ebenso E.E., Obi-Egbedi N.O., *Desalination*, 2009, **247**:561 [Crossref], [Google Scheme], [Publisher]
[27]. Singh, A., Ahamad I., Quraishi M.A., *Arab. J. Chem.*, 2016, **9**:S1584 [Crossref], [Google Scheme], [Publisher].
[28]. El-Etre A., *Corros. Sci.*, 2003, **45**:2485 [Crossref], [Google Scheme], [Publisher]
[29]. Desselberger U., *J. Infect.*, 2000, **40**:3 [Crossref], [Google Scheme], [Publisher]
[30]. Allaker, R.P., *J. Dent. Res.*, 2010, **89**:1175 [Crossref], [Google Scheme], [Publisher]
[31]. Roselli, M., Finamore A., Garaguso I., Britti M.S., Mengheri E., *J. Nutr*, 2003, **133**:4077 [Crossref], [Google Scheme], [Publisher]
[32]. Subashini K., Prakash S., Sujatha V., *Mater. Res. Express*, 2020, **7**:115308 [Crossref], [Google Scheme], [Publisher]

HOW TO CITE THIS ARTICLE
Rawaa Abbas Mohammed, Khulood A. Saleh. Conducting Poly [*N*-(4-Methoxy Phenyl) Maleamic acid]/Metals Oxides Nanocomposites for Corrosion Protection and Bioactivity Applications, *Chem. Methodol.*, 2022, 6(1) 74-82
DOI: 10.22034/chemm.2022.1.8
URL: http://www.chemmethod.com/article_139638.html